# Simulation of Container Ship in Shallow Water at Model Scale and Full Scale

Ganbo Deng, Emmanuel Guilmineau, Alban Leroyer, Patrick Queutey, Michel Visonneau, Jeroen Wackers

# Simulation of Container Ship in Shallow Water at Model Scale and Full Scale

G.B. Deng, E. Guilmineau, A. Leroyer, P. Queutey, M. Visonneau, and J. Wackers

*LHEEA, Ecole Centrale de Nantes,44321,France*

Tel: 33 240371648, e-mail: Ganbo.deng@ec-nantes.fr

## Abstract

Although CFD computation can predict resistance for conventional vessels with reliable accuracy at deep water condition, its predictive capability at shallow water condition is still unclear. One of the main objective of this study is to assess the accuracy of CFD computation for this kind of configuration and attempt to identify physical phenomena poorly modeled in the simulation. Shallow water resistance and squat are predicted for two different ship models, namely the DTC container ship, and the KVLCC2 tanker. Numerical uncertainty related to grid density, turbulence model as well as near wall turbulence model treatment will be investigated. Computation at full scale is also performed for the container ship to check the scale effect in ship squat prediction.

## 1. Introduction

Although CFD computation can predict resistance for conventional vessels with reliable accuracy at deep water condition, its predictive capability at shallow water condition is still unclear. While ship resistance and propulsion are the major concerns in deep water condition, squat prediction is also of crucial importance in shallow water condition for safety reason. The main objective of this study is to assess the accuracy of CFD simulation for ship resistance and squat in shallow water and attempt to identify physical phenomena poorly modeled in numerical simulation. The main sources in shallow water prediction is turbulence modelization. Unlike in deep water, flow usually separates in shallow water condition. It is well known that the accuracy of turbulence model employed in RANSE approach is questionable when flow separation occurs. Reliable experimental data and careful CFD validation works are required to assess the predictive capability of CFD simulation for such configuration. During NATO AVT-163 research project, Toxopeus et al. [7] have compared CFD prediction with different codes for ship resistance for the KVLCC2 tanker at different water depths. Although CFD predictions with different codes agree fairly well with measurement data for deep water configuration, more discrepancies are observed in shallow water configuration compared with measurement data provided by INSEAN for two different water depths. CFD simulation show that while the effect of free surface on ship resistance is about 3% for the low Froude number considered

(Fr=0.064), 10% difference can be observed in shallow water condition. At very shallow water condition h/T=1.2 (h and T are water depth and draft respectively), CFD simulation over predicts the resistance by about 4-5% when free-surface and tank width are taken into account, while at moderate shallow water condition (h/T=1.5), about 10% under prediction is observed. Those contradictory predictions make it difficult to draw a clear conclusion. As the measurement is done with a false bottom at INSEAN, it is preferable to use measurement data obtained with a shallow water towing tank for CFD validation. During the preparation for the SIMMAN 2014 Workshop [6] devoted to ship maneuvering, new experimental works for the same hull form have been conducted by two different organizations, namely the Bulgarian Ship Hydrodynamics Center (BSHC), and the Flanders Hydraulics Research (FHR). Another newly available shallow water experimental data is provided by the Development Center for Ship Technology and Transport Systems (DST) and by the Federal Waterways Engineering and Research Institute (BAW) for the Post-Panamax type container vessel Duisburg Test Case (DTC, CAD data available at http://www.unidue.de/IST/ismt_presquat4.shtml). The under-keel clearance (UKC) for the DTC test case is even smaller (h/T=1.143). It is used as test case for the pre-squat workshop [4]. Those new experimental data obtained in shallow water towing tank provide valuable data for CFD validation. The objective of the present paper is therefore to validate CFD prediction for shallow water configuration by comparing with those newly publicly available experimental data.

## 2. Flow Solver

Our in house solver ISIS-CFD, available as a part of the FINE™/-Marine computing suite, is an incompressible unsteady Reynolds-averaged Navier-Stokes (URANS) method. The solver is based on the finite volume method to build the spatial discretization of the transport equations. The unstructured discretization is face-based. While all unknown state variables are cell-centered, the systems of equations used in the implicit time stepping procedure are constructed face by face. Fluxes are computed in a loop over the faces and the contribution of each face is then added to the two cells next to the face. This technique poses no specific requirements on the topology of the cells. Therefore, the grids can be completely unstructured; cells with an arbitrary number of arbitrarily-shaped faces are accepted. Pressure-velocity coupling is obtained through a Rhie & Chow SIMPLE type method: at each time step, the velocity updates come from the momentum equations and the pressure is given by the mass conservation law, transformed into a pressure equation. In the case of turbulent flows, transport equations for the variables in the turbulence model are added to the discretization. Free-surface flow is simulated with a multi-phase flow approach: the water surface is captured with a conservation equation for the volume fraction of water, discretized with specific compressive discretization schemes[5]. The method features sophisticated turbulence models: apart from the classical two-equation k-ε and k-ω models, the anisotropic two-equation Explicit Algebraic Stress Model (EASM), as well as Reynolds Stress Transport Models, are available[1]. The technique

included for the 6 degrees of freedom simulation of ship motion is described by Leroyer & Visonneau [2]. Time-integration of Newton's law for the ship motion is combined with analytical weighted or elastic analogy grid deformation to adapt the fluid mesh to the moving ship. Parallelization is based on domain decomposition. The grid is divided into different partitions; these partitions contain the cells. The interface faces on the boundaries between the partitions are shared between the partitions; information on these faces is exchanged with the MPI (Message Passing Interface) protocol. This method works with the sliding grid approach and the different sub-domains can be distributed arbitrarily over the processors. Finally, a parallelized anisotropic automatic grid refinement procedure with dynamic load balancing is implemented and controlled by various flow-related criteria.

## 3. Numerical Simulation

### 3.1 Ship models

The first test case is the DTC container ship. Its main characteristics are given in table 1. The experiment is conducted in a towing tank with a rectangular cross section (10m width and 0.4m water depth) at DST both for ship resistance and squat, while measurement for ship squat only has also been performed at BAW in an asymmetric channel. The model was free to trim and heave. The rudder was appended. The test was conducted for five different speeds at DST.

| | Full scale | Model scale |
|---|---|---|
| Length $L_{wl}$ [m] | 360.79 | 9.02 |
| Beam B [m] | 51 | 1.275 |
| Draught T [m] | 14 | 0.35 |
| Volume V [$m^3$] | 165804 | 2.591 |
| Wetted Surface [$m^2$] | 21560 | 13.475 |

Table 1: Main particulars of DTC for both full scale and model scale ship.

The second test case is the well known KVLCC2 tanker. The main characteristics of this ship model can be easily found in the literature and will not be repeated here. Measurement with a ship model with scale factor of 1/45.714 (Lpp=7m) has been conducted in BSHC in a towing tank with 16m width, while FHR performs a measurement with a smaller ship model with scale factor of 1/75 (Lpp=4.2667m) in a towing tank with 7m width. The Froude number Fr=0.064 and water height h/T=1.2 are the same in both measurements.

### 3.2 Mesh generation and case setup

The computational domain is a parallelepiped. A half boat configuration with mirror

boundary condition is employed. Whole domain computation has been performed for verification. It has been found that due to separation, the predicted flow is not always symmetric. Either a vortex shedding unsteady solution or an asymmetric steady solution can be obtained. But in both cases, the influence on ship resistance and squat is very small. Hence, to save computational time, all results presented in this paper are obtained with a half-domain computation. The domain width is the same as the towing tank. The height of the computational domain is about 0.5 Lpp. It starts at 1.6 Lpp before the hull and extends at 2.2Lpp after the hull. The mesh is generated with the unstructured hexahedral mesh generator Hexpress™. Far field boundary condition is applied at the inlet and outlet boundaries. Slip wall condition is applied to the side wall. Pressure boundary condition is applied to the top boundary. Attention needs to be given concerning the boundary conditions applied to the hull and to the bottom wall. For the hull, wall function approach is accurate enough for resistance computation under deep water condition. It is commonly used in routine computation for industrial application to save computational resources. Our experiences show that the validation of wall function approach under shallow water condition is questionable. Hence, in the present study, computation will be performed both with wall function and with low Reynolds number model for the hull, and the results will be compared. Slipping boundary condition is usually applied to the bottom wall. However, under very shallow water condition, boundary layer may develop at the bottom wall. We also compare two different near wall treatments for the bottom wall in the present study, one with slipping boundary condition, and the other one with wall function. This leads to three different setups shown in table 2, where number of cells for different cases are also given for the DTC test case.

Table 2. Different setup for near wall treatment

| Setup | WF-SLIP | LRN-SLIP | LRN-WF |
|---|---|---|---|
| Hull | Wall function | No slip | No slip |
| Bottom wall | Slip | slip | Wall function |
| Number of cells | 1456000 | 3091000 | 3048000 |

WF: wall function; SLIP: sliping boundary condition; LRN: Low Renolds number

### 3.3 Grid dependency study

Grid dependency study is performed for the DTC test case with v=0.791m/s. Table 3 shows the predicted ship resistance, trim, sinkage as well as number of cells for different grids. The SST model is employed for this study with the WF-SLIP type boundary condition indicated in table 2. The extrapolated value as well as the observed order of convergence obtained with Richardson extrapolation is also given when a monotonic convergence behavior is observed. Monotonic convergence behavior is not observed for the resistance. However, data range is very small (less than 0.5%), which

indicates that the mesh is fine enough. Nearly second order convergence is observed for the sinkage. Estimated numerical uncertainty for the sinkage is about 0.2%. The observed order of convergence for the trim angle is too small (p=0.32). Hence, extrapolation is obtained with an assumed second order of convergence. Reliable uncertainty estimation is difficult when the observed order of convergence is too small. But we believe that it is smaller than 10%. It should be noticed that numerical simulation predicts a bow down position, while the measurement indicates a bow up position. All other computations performed in the present study have a grid density similar to the medium grid. The difference in terms of number of grid cells for different setup is due to near wall boundary layer only.

| Grid | Nb of cells | Resistance(N) | Sinkage (mm) | Trim(deg) |
|---|---|---|---|---|
| Exp. | | 29.39 | 11.8 | -0.01 |
| Coarse | 857275 | 27.04 | 13.815 | 0.0132 |
| Medium | 1772265 | 26.92 | 13.796 | 0.0126 |
| Fine | 3199165 | 27.00 | 13.787 | 0.0122 |
| Extrap. | | x | 13.771 | 0.0118(*) |
| Order | | x | 1.9 | 0.32 |

Table 3: Grid dependency study.

(*): extrapolation with 2nd order accuracy

**3.4 Resistance prediction for the DTC test case**

Computation has been performed both with the SST model and with the EASM model. Table 4 summarizes the predicted resistance for different cases. Comparison with measurement result is shown in figure 1. To make the comparison easier, table 5 gives the relative difference in percentage compared with the mean value for each speed. By comparing column 2 and 3 in table 5, it can be seen that applying wall function at the hull results into an under-estimation of ship resistance by about 3%. Hence, wall function approach is not suitable for shallow water prediction. Divergence occurs in the computation with WF-SLIP setup due to severe grid deformation for the two highest speeds. Mesh quality needs to be improved. As the resistance is under estimated with this setup, no attempt is made to generate a new mesh for those two cases. Comparison between column 3 and 4 reveals that applying wall function instead of slip boundary condition at the bottom wall also increase the resistance by about 1-2% except for the case with the lowest speed. Hence, for such low UKC, boundary layer at the bottom wall needs to be taken into account in the simulation. Finally, the comparison between the last two columns shows that the effect of turbulence modelization is important. With the EASM model, the predicted resistance is about 3-5% higher. The effect is more important in low speed than in high speed. Such sensitivity to turbulence modelization can be explained by the fact the flow separation is observed at the stern. It is well known that statistical turbulence modelization with

RANSE approach is unable to provide accurate prediction when flow separation occurs. Validation with experimental data is required to access the accuracy of the two turbulence models employed in the present study. Table6 provides the predicted friction resistance. For comparison, friction resistance given by ITTC 57 formula is also provided. From this table, it can be seen that friction resistance prediction is less sensitive to different near wall treatment and turbulence modelization. Moreover for all speeds, friction resistance is about 20% higher than the ITTC value. Such high friction resistance also suggests that usual full scale ship resistance extrapolation procedure is unlikely valid for shallow water configuration.

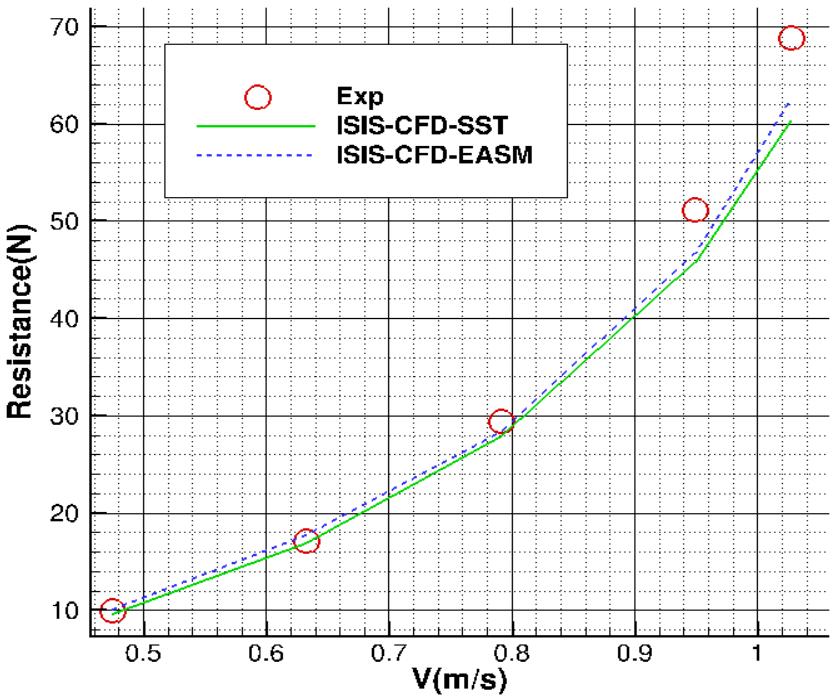


Figure 1. Resistance prediction for different speeds

| | SST | | | EASM |
|---|---|---|---|---|
| V [m/s] | WF-SLIP | LRN-SLIP | LRN-WF | LRN-WF |
| 0.475 | 9.41 | 9.57 | 9.60 | 10.01 |
| 0.632 | 16.22 | 16.71 | 16.9 | 17.70 |
| 0.791 | 26.45 | 27.28 | 27.85 | 28.35 |
| 0.949 | / | 45.06 | 45.74 | 46.70 |
| 1.027 | / | 59.66 | 60.42 | 62.65 |

Table 4: Predicted resistance (N) for different cases

WF: Wall-Function, LRN:Low Reynolds Number, SLIP: slipping wall

| | | SST | | | EASM |
|---|---|---|---|---|---|
| V [m/s] | Mean | WF -SLIP | LRN-SLIP | LRN-WF | LRN-WF |
| 0.475 | 9.67 | -2.6 % | -1.0% | -0.7% | 4.0% |
| 0.632 | 16.88 | -3.9 % | -1.0% | 0.1% | 4.9% |
| 0.791 | 27.40 | -3.3 % | -0.4% | 1.6% | 3.6% |
| 0.949 | 45.83 | / | -1.6% | -0.2% | 1.8% |
| 1.027 | 60.90 | / | -2.0% | -0.7% | 2.8% |

Table 5: Relative difference compared with mean value

| V [m/s] | ITTC 57 | SST | | | EASM |
|---|---|---|---|---|---|
| | | WF-SLIP | LRN-SLIP | LRN-WF | LRN-WF |
| 0.475 | 5.35 | 6.33 | 6.37 | 6.23 | 6.35 |
| 0.632 | 8.98 | 10.67 | 10.87 | 10.68 | 11.06 |
| 0.791 | 13.51 | 16.43 | 16.68 | 16.36 | 16.62 |
| 0.949 | 18.82 | / | 23.31 | 22.72 | 23.07 |
| 1.027 | 21.74 | / | 26.58 | 25.86 | 26.15 |

Table 6: Predicted friction resistance (N) for different cases

WF: Wall-Function, LRN:Low Reynolds Number, SLIP: slipping wall

**3.5 Ship squat prediction for the DTC test case**

Unlike for the resistance, sinkage is not sensitive to different near wall treatments and turbulence modelizations. Predicted results predicted with LRN-WF near wall treatment is given in table 7. Comparison with measurement data for sinkage at bow and at stern are shown in figure 2 and 3. Model scale measurement for sinkage is usually scaled to full scale as full scale squat estimation. To evaluate scale effect in ship squat, a full scale computation has been performed. Wall function is applied at the hull in those computations with y+ value about 50. All computations have been performed with a symmetric channel, while measurement data both for the symmetric channel and for the asymmetric channel are included in the figures for comparison. The geometry of the asymmetric channel can be found in [4]. CFD prediction at model scale agrees with measurement data globally both at the bow and at the stern. Scale effect is not negligible. At model scale, the predicted trim angle increases with ship speed up to v=9.7 knots. Then, it decreases from a maximum bow down position at v=9.7 knots to a bow up position at v=12.6 knots. At full scale, predicted trim angle keeps increasing with bow down position. Sinkage at bow is more important, while a smaller value is observed at stern.

| V [m/s] | Sinkage(mm) | Trim(deg) | |
|---|---|---|---|
| | | SST | EASM |
| 0.475 | 5.55 | 0.00465 | 0.00465 |
| 0.632 | 8.84 | 0.0077 | 0.0077 |
| 0.791 | 13.78 | 0.011 | 0.0109 |
| 0.949 | 21.15 | 0.0089 | 0.0073 |
| 1.027 | 26.18 | -0.00075 | -0.00583 |

Table 7: Predicted trim (positive bow down) and sinkage for different speed

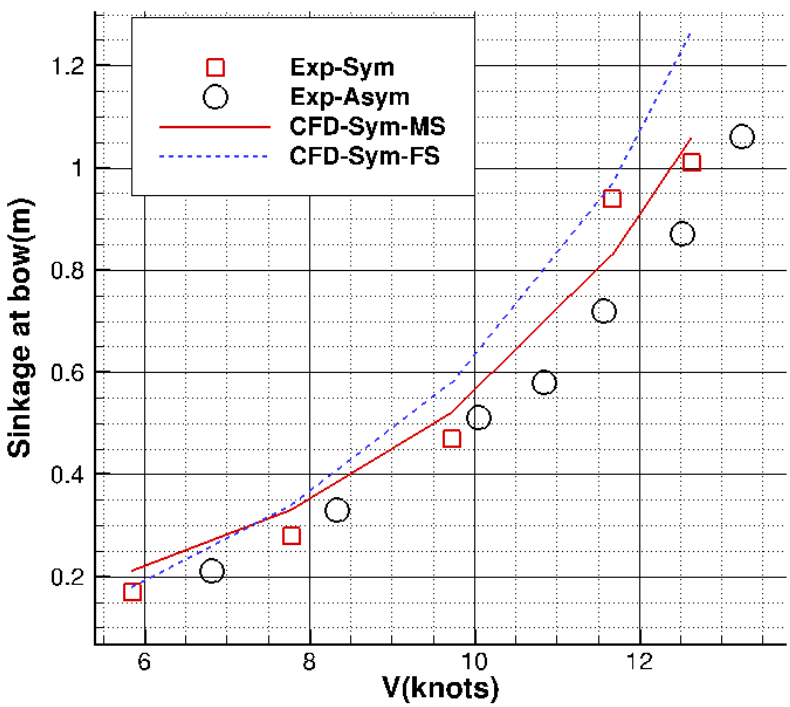


Figure 2. Predicted sinkage at bow

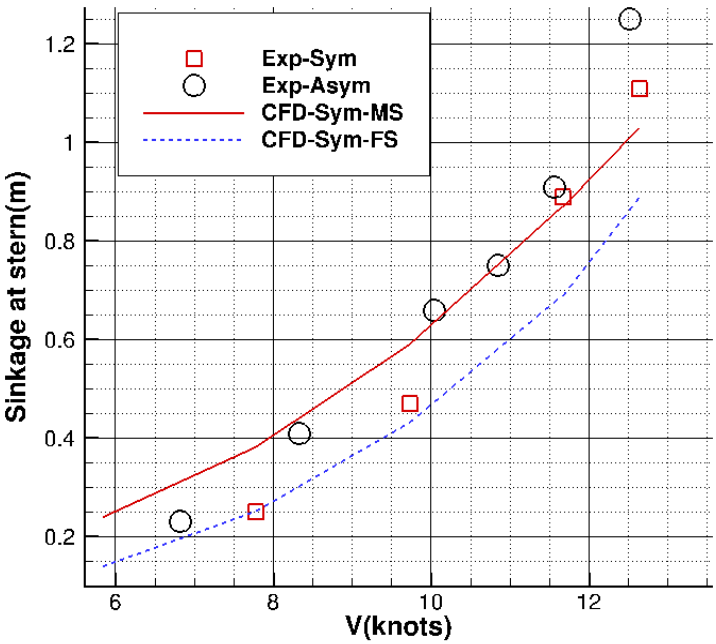


Figure 3. Predicted sinkage at stern

### 3.6 Numerical prediction for the KVLCC2 test case

The configuration for the KVLCC2 geometry corresponds to the experimental setup at BSHC with h/T=1.2, draft=0.455m and Lpp=7m. The resistance measurement has been conducted with a bare hull geometry. Computation has been performed with $0.4U_0$, $0.6U_0$, $0.8U_0$, $1.0U_0$, $1.13U_0$ and $1.32U_0$, $U_0$ = 0.532m/s being the reference velocity proposed for the SIMMAN 2014 workshop for this configuration. Froude number ranges from 0.0257 to 0.0847. Grid dependency study was not performed for this test case. Mesh density is similar to the DTC test case. The EASM model is used. Low Reynolds number model is applied at the hull, while wall-function is applied to the bottom wall. Figure 4 compares ship resistance with measurement data. Unlike the DTC test case, good agreement is observed for the entire speed range. Sinkage at bow and stern is compared with measurement data in figures 5 and 6. More discrepancies are observed compared with resistance prediction. While ship resistance depends mainly on dynamic forces acting on the boat, sinkage depends on free-surface position that relies both on dynamic pressure as well as hydraulic effect due to ship advancing motion.. As the predicted ship resistance agrees well with the measurement data, we believe that the predicted dynamic forces are not responsible for the discrepancies observed on the sinkage. At low speed, we are certain that the predicted dynamic forces are such that the boat should sink at mid ship position, rather than the near zero sinkage as observed in the measurement. If the difference between CFD prediction and the measurement data is not due to measurement uncertainty, the only possible explanation is that the variation of water level in the real towing tank can not be

correctly simulated by CFD computation in which numerical towing tank is opened both in front and behind the ship. Such variation of water level is a hydraulic effect rather than a dynamic effect. Moreover, mesh density in the water channel is relatively coarse. Further investigations both in CFD and in the measurement are therefore required to assess the accuracy of CFD prediction for ship squat in shallow water.

| | Scale factor | Channel Width | Exp (N) | ISIS-CFD (N) | Error |
|---|---|---|---|---|---|
| BSHC | 45.71 | 16m | 13.29 | 13.39 | 0.8% |
| INSEAN | 45.71 | 9m | 14.44 | 15.07 | +4.4% |
| FHR | 75 | 7m | 3.615 | 3.447 | -4.6% |

Table 8. Ship resistance for the KVLCC2 test case at h/T=1.2

Ship resistance predictions for the KVLVCC2 test case with the same water high h/T=1.2 and the same Froude number Fr=0.0642 are compared for different configurations in table 8. The three cases differ by the channel width and scale factor. Good agreement is observed for the BSHC configuration. For INSEAN configuration, CFD prediction is 4.4% higher than the measurement. We believe that the over-prediction in CFD is due to the fact that we use a true bottom wall with 9m width in the computation, while in INSEAN's measurement, the width of the bottom wall is only 7.5 meters in a deep water tank with 9 meters width. For the FHR configuration, smaller ship model might be responsible for the under-estimation observed in CFD prediction due to the effect of turbulence stimulator. Higher relative error might also be the consequence of smaller resistance value.

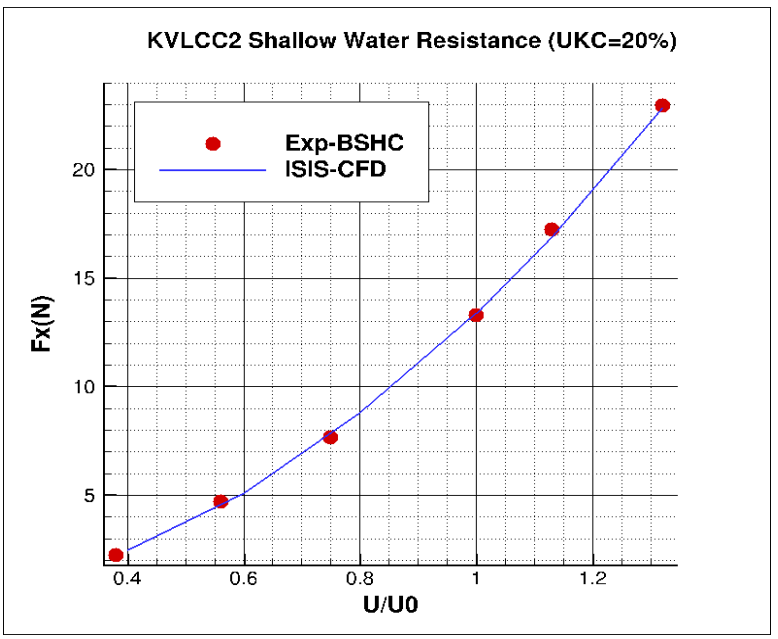


Figure 4. Resistance prediction for the KVLCC2 test case.

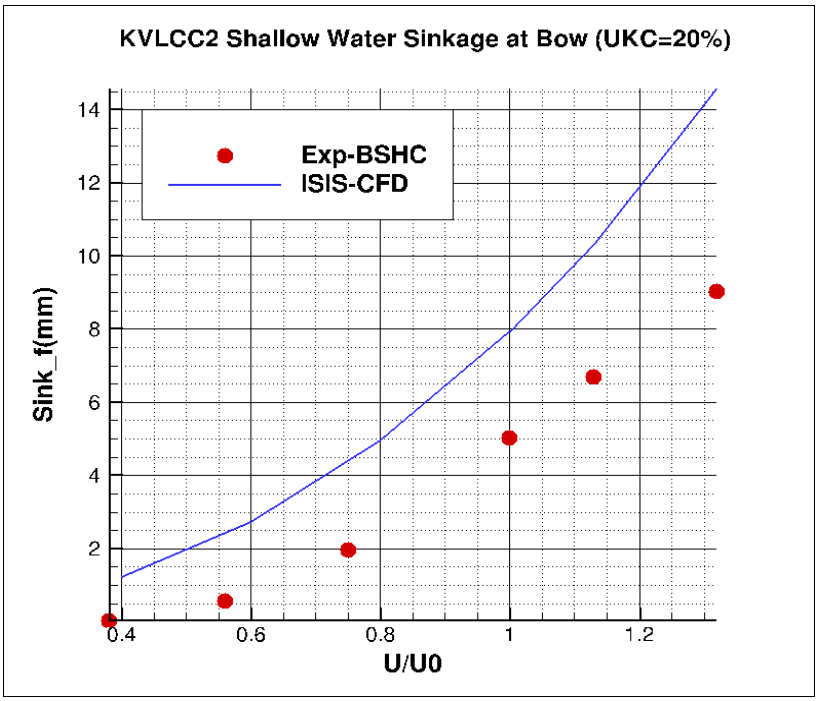


Figure 5. Predicted sinkage at bow

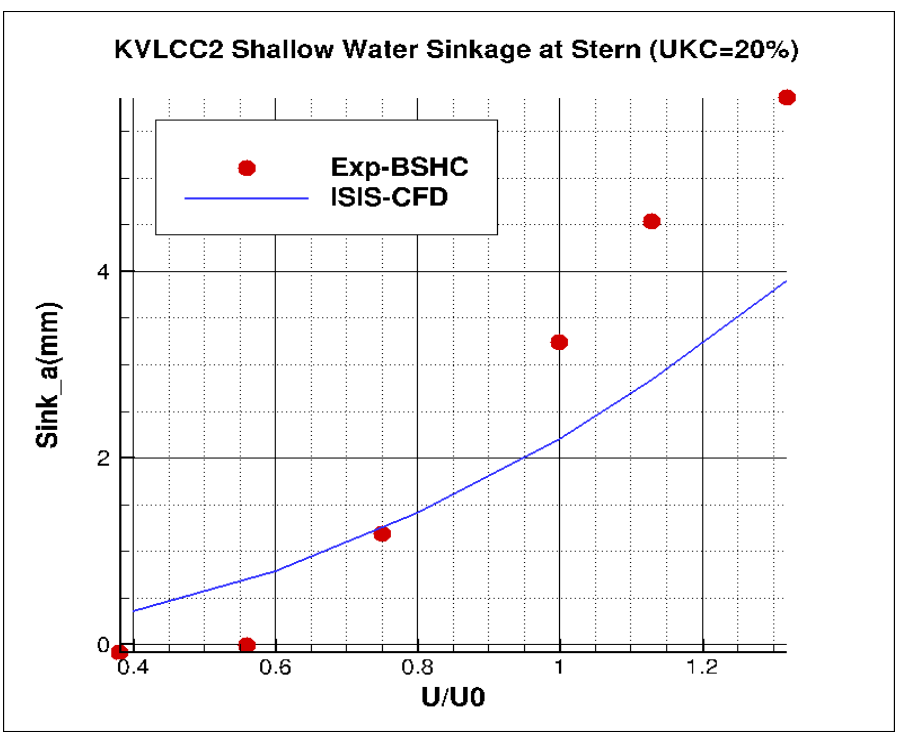


Figure 6. Predicted sinkage at stern.

## 4. Conclusions

In this paper, RANSE simulation is performed for the DTC container ship and the KVLCC2 tanker advancing in shallow water. Good prediction for ship resistance is observed for the KVKCC2 test case, while discrepancies still exists for the DTC test case. Numerical prediction reveals that accurate prediction requires the use of low Reynolds turbulence model. Boundary layer developed at the bottom wall needs to be taken into account. It has also been found that turbulence modeling plays an important role due to flow separation at the stern. Resistance predicted by the EASM model is about 3-5 % higher than the SST model. More discrepancies are observed in ship squat prediction. It is argued that such discrepancies are more likely due to water level in numerical towing tank rather than due to poor prediction of dynamic forces.

## Acknowledgments

This work was granted access to the HPC resources of IDRIS and CINES under the allocation 2013-21308 and 2014-21308 made by GENCI (Grand Equipement National de Calcul Intensif). Part of the computation has been performed by Nour Yahfoufi during her internship. The authors are grateful to Professor E. Milanov and V. Chotukova for their permission to publish their experimental result. We are also in debt with Dr. Phillipp Mucha for having provided us with the measurement data for the DTC test case.

## References

[1] Deng, G. , and Visonneau, M., 1999. “Comparison of explicit algebraic stress models and second-order turbulence closures for steady flow around ships”. In 7th Symposium on Numerical Ship Hydrodynamics, pp. 4.4–1–4.4–15.

[2] Leroyer, A., and Visonneau, M., 2005. “Numerical methods for RANSE simulations of a self-propelled fish-like body”. Journal of Fluids and Structures, 20, pp. 975–991.

[3] el Moctar O., Shigunov, V., and Zorn, T., 2012. “Duisburg test case: Post-Panamax container ship for benchmarking”. Ship Technology Research Journal, 59, pp. 50–64.

[4] Pre-squat workshop, http://www.unidue.de/IST/ismt_presquat.shtml

[5] Queutey, P., and Visonneau, M., 2007. “An interface capturing method for free-surface hydrodynamic flows”. Computers and Fluids, 36, pp. 1481–1510.

[6] SIMMAN 2014 Workshop, www.simman2014.dk

[7] Toxopeus, S. L., Simonsen, C. D., Guilmineau, E., Visonneau, M., Xing, T., Stern, F., “Investigation of water depth and basin wall effects on KVLCC2 in manoeuvring motion using viscous-flow calculations”, J Mar Sci Technol, 11 May 2013, DOI 10.1007/s00773-013-0221-6